2003-07-03

Experimental and Calculated Stark Widths Within the Kr I Spectrum

Vladimir Milosavljevic
Technological University Dublin, vm@tudublin.ie

Stevan Djenize
Faculty of Physics, University of Belgrade, Serbia

Milan S. Dimitrijevic
University of Belgrade

Recommended Citation

V. Milosavljevic, et al., Experimental and calculated Stark widths within the Kr I spectrum. *Physical Review* E68, July (2003). doi:10.1103/PhysRevE.68.016402

Experimental and calculated Stark widths within the Kr I spectrum

V. Milosavljević* and S. Djeniže†
Faculty of Physics, University of Belgrade, P.O.B. 368, Serbia, Yugoslavia

M. S. Dimitrijević‡
Astronomical Observatory, Belgrade, Volgina 7, Serbia, Yugoslavia
(Received 14 January 2003; published 3 July 2003)

On the basis of the precisely recorded 20 neutral krypton (Kr I) line shapes (in the $5s$-$5p$ and $5s$-$6p$ transitions), we have obtained the basic plasma parameters, i.e., electron temperature (T) and electron density (N) using our line deconvolution procedure in a plasma created in a linear, low-pressure, pulsed arc discharge operated in krypton. The mentioned plasma parameters have also been measured using independent experimental diagnostics techniques. Agreement has been found among the two sets of the obtained parameters. This recommends our deconvolution procedure for plasma diagnostical purposes, especially in astrophysics where direct measurements of the main plasma parameters (T and N) are not possible. On the basis of the observed asymmetry of the Stark broadened line profile, we have obtained not only its ion broadening parameter (A) which is caused by influence of the ion-microfield over the line broadening mechanism but also the influence of the ion-dynamic effect (D) over the line shape. The separate electron (W_e) and ion (W_i) contributions to the total Stark width, which have not been measured so far, have also been obtained. Stark widths are calculated using the semiclassical perturbation formalism for electrons, protons, and helium ions as perturbers.

DOI: 10.1103/PhysRevE.68.016402 PACS number(s): 52.25.Ya, 32.70.Jz, 52.70.Kz

I. INTRODUCTION

Due to the development of space born astronomical techniques and devices such as Goddard high resolution spectrograph on the Hubble space telescope the spectral lines of trace elements, such as krypton, are observed and the corresponding atomic data are of increasing interest. Krypton has been detected in the spectra of the interstellar medium [1,2], which represents the material from which the young early type stars (as, e.g., Ap and Bp type stars where Stark broadening data are of interest) are formed [3]. On the basis of the recent investigation of the planetary nebula spectra [4] it was found that krypton is one of the most abundant elements in the cosmos with $Z>32$. Moreover, krypton is present in many light sources and lasers as the working gas. If the Stark broadening is the principal pressure broadening mechanism in plasmas (with 10^{21}–10^{25} m^{-3} electron density), it is possible to obtain from Stark width values other basic plasma parameters as, e.g., electron temperature (T) and density (N). Consequently, the knowledge of the Stark width of the krypton spectral lines is of interest for plasma diagnostical purposes.

Seven experimental works [5–11] are devoted to the neutral krypton (Kr I) Stark width investigation. In experiments performed up to now the symmetrical Voigt or Lorentz line profiles were used for deconvolution procedure giving *a priori* overvalued Stark width values (W_e) generated by electrons without any possibility to estimate the ion component (W_i) generated by Kr II ions (or other ions) [12–14] in the total Stark width (W_t).

Our W_e and W_i values, presented here for 20 Kr I lines, are separated from measured total Stark width using the line deconvolution procedure described in Refs. [15,16] which have already been applied for some He I [17,18] and Ne I [19] lines. On the basis of the observed line profile asymmetry we have obtained the role of the quasistatic ion (A) and ion-dynamic effect (D) in the line broadening mechanism. To the knowledge of the authors no experimental W_t, W_i, and D values and no theoretical W_e and A values exist.

Using the semiclassical perturbation formalism (SCPF) (updated several times) [20–25], as the first, we have calculated W_e values for 11 Kr I lines and W_i values, also, generated by protons and helium ions which are the main components in the astrophysical plasmas.

The basic plasma parameters, i.e., electron temperature (T^D) and electron density (N^D) have also been obtained by using our line deconvolution procedure. To the knowledge of the authors, our T and N values are data results obtained directly from the line profile, using deconvolution procedure. Plasma parameters have also been measured (T^{expt} and N^{expt}) using independent, well-known, experimental diagnostical techniques. Very good agreement was found among the two sets of the obtained parameters (T^D and T^{expt}; and N^D and N^{expt}). This recommends our deconvolution procedure for plasma diagnostical purposes, especially in astrophysics where direct measurements of the main plasma parameters (T and N) are not possible.

II. EXPERIMENT

The modified version of the linear low-pressure pulsed arc [26,27] has been used as a plasma source. A pulsed discharge was performed in a quartz discharge tube of 5-mm inner diameter and plasma length of 7.2 cm. The tube has end-on quartz window. On the opposite side of the electrodes the

*Electronic address: vladimir@ff.bg.ac.yu
†Electronic address: steva@ff.bg.ac.yu
‡Electronic address: mdimitrijevic@aob.bg.ac.yu

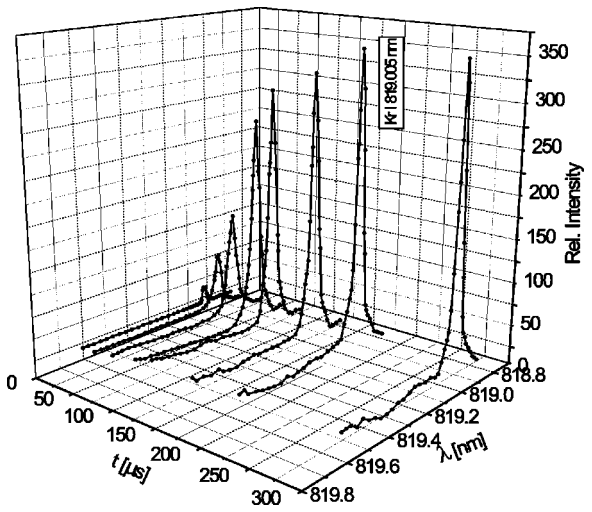

FIG. 1. Temporal evolution of the 819.005-nm Kr I spectral line profile during the plasma decay.

glass tube was expanded in order to reduce erosion of the glass wall and also sputtering of the electrode material onto the quartz windows. The working gas was pure krypton at 130 Pa filling pressure in flowing regime. Spectroscopic observation of isolated spectral lines has been made end-on along the axis of the discharge tube. A capacitor of 14 μF was charged up to 1.5 kV. The line profiles were recorded using a shot-by-shot technique with a photomultiplier (EMI 9789 QB and EMI 9659B) and a grating spectrograph (Zeiss PGS-2, reciprocal linear dispersion 0.73 nm/mm in first order) system. The instrumental full width at half maximum-(FWHM) of 8 pm was determined by using the narrow spectral lines emitted by the hollow cathode discharge. The recorded profiles of these lines are Gaussian in shape within 8% accuracy within the range of the investigated spectral line wavelengths. The spectrograph exit slit (10 μm) with the calibrated photomultiplier was micrometrically traversed along the spectral plane in small wavelength steps (7.3 pm). The averaged photomultiplier signal (five shots at the same spectral range) was digitized using an oscilloscope, interfaced to a computer. A sample output, as example, is shown in Fig. 1.

The absence of self-absorption was checked by using the technique described in Ref. [28]. Diagnostical methods and used procedures have been described, in detail, in our earlier work [27]. Thus, electron temperature (T^{expt}) decay is obtained by using the Saha equation applied for Kr II and Kr I line intensity ratios. Electron density (N^{expt}) decay is obtained using laser interferometry technique. Temporal evolutions of T^{expt} and N^{expt} are presented in Fig. 2, together with averaged T^{D} and N^{D} values obtained using line deconvolution procedure (see Sec. IV).

III. THEORETICAL BACKGROUND

The total line Stark FWHM (full width at a half intensity maximum, W_{t}) is given as

$$W_{\mathrm{t}} = W_{\mathrm{e}} + W_{\mathrm{i}}, \tag{1}$$

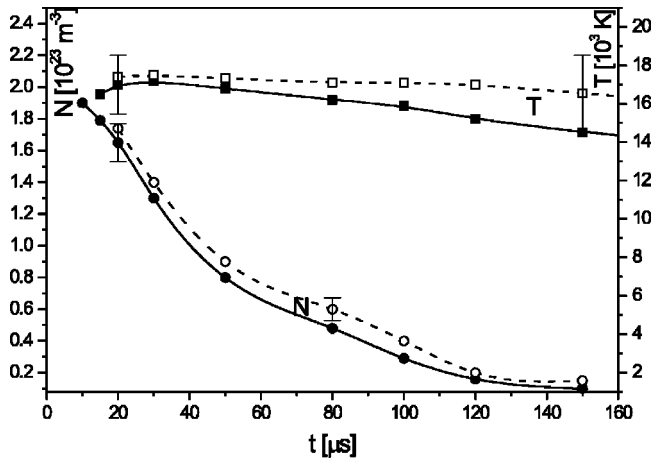

FIG. 2. Electron temperature (T) and density (N) decays. Full lines represent measured data using independent experimental techniques. Dashed lines represent averaged (within 20 Kr I lines) plasma parameters obtained using our line deconvolution procedure. Error bars represent estimated accuracies of the measurements ($\pm 11\%$ and $\pm 7\%$ for T and N, respectively) and deconvolutions ($\pm 12\%$).

where W_{e} and W_{i} are the electron and ion contributions, respectively. For a nonhydrogenic, isolated neutral atom line the ion broadening is not negligible and the line profiles are described by an asymmetric K function [see Eq. (6) in Sec. IV and in Ref. [15]]. The total Stark width (W_{t}) [29–31] may be calculated from the equation

$$W_{\mathrm{t}} \approx W_{\mathrm{e}}[1 + 1.75AD(1 - 0.75R)], \tag{2}$$

where

$$R = \sqrt[6]{\frac{36\pi e^6 N}{(kT)^3}} \tag{3}$$

is the ratio of the mean ion separation to the Debye length. N and T represent electron density and temperature, respectively. A is the quasistatic ion broadening parameter [see Eq. (224) in Ref. [29]] and D is a coefficient of the ion-dynamic contribution with the established criterion

$$D = \frac{1.36}{1.75(1-0.75R)} B^{-1/3} \quad \text{for} \quad B < \left(\frac{1.36}{1.75(1-0.75R)} \right)^3;$$

or

$$D = 1 \quad \text{for} \quad B \geqslant \left(\frac{1.36}{1.75(1-0.75R)} \right)^3, \tag{4}$$

where

$$B = A^{1/3} \frac{4.03 \times 10^{-7} W_{\mathrm{e}}(\mathrm{nm})}{[\lambda\ (\mathrm{nm})]^2} [N(\mathrm{m}^{-3})]^{2/3} \sqrt{\frac{\mu}{T_g\,(K)}} < 1 \tag{5}$$

is the factor with atom-ion perturber reduced mass μ (in amu) and gas temperature T_g. When $D = 1$ the influence of

the ion-dynamic effect is negligible and the line shape is treated using the quasistatic ion approximation. From Eqs. (1)–(6) it is possible to obtain the plasma parameters (N and T) and the line broadening characteristics (W_t, W_e, W_i, A, and D). One can see that the ion contribution, expressed in terms of the A and D parameters directly determines the ion width (W_i) component in the total Stark width [Eqs. (1) and (2)].

IV. NUMERICAL PROCEDURE FOR DECONVOLUTION

The proposed functions for various line shapes [Eq. (6)] is of the integral form and include several parameters. Some of these parameters can be determined in separate experiments, but not all of them. Furthermore, it is impossible to find an analytical solution for the integrals and methods of numerical integration to be applied. This procedure, combined with the simultaneous fitting of several free parameters, causes the deconvolution to be an extremely difficult task and requires a number of computer supported mathematical techniques. Particular problems are the questions of convergence and reliability of deconvolution procedure, which are tightly connected with the quality of experimental data,

$$K(\lambda)=K_o+K_{\max}\int_{-\infty}^{\infty}\exp(-t^2),$$

$$\left[\int_0^{\infty}\frac{H_R(\beta)}{1+\left(2\dfrac{\lambda-\lambda_o-(W_G/2\sqrt{ln2})t}{W_e}-\alpha\beta^2\right)^2}d\beta\right]dt. \tag{6}$$

Here K_o is the baseline (offset) and $K_{\max}$ is the maximum of intensity (intensity for $\lambda=\lambda_o$) [15]. $H_R(\beta)$ is an electric microfield strength distribution function of normalized field strength $\beta=F/F_o$, where F_o is the Holtsmark field strength. A ($\alpha=A^{4/3}$) is the static ion broadening parameter as a measure of the relative importance of ion and electron broadenings. R is the ratio of the mean distance between the ions to the Debye radius, i.e., the Debye shielding parameter and W_e is the electron width (FWHM) in the $j_{A,R}$ profile [see Eq. (7)].

For the purpose of deconvolution iteration process we need to know the value of K function as a function of λ for every group of parameters ($K_{\max}$, λ_o, W_e, W_G, R, A). The function $K(\lambda)$ is in integral form and we have to solve a triple integral in each step of iteration process of varying the above group of parameters. The first integral in the K function is the microfield strength distribution function $H_R(\beta)$, the second one is the $j_{A,R}(\lambda)$ function [Eq. (7)], and the third is the convolution integral of a Gaussian and a plasma broadened spectral line profile $j_{A,R}(\lambda)$, denoted by $K(\lambda)$ [Eq. (6)]. All these integrals have no analytic solution and must be solved using the numerical integration,

$$j_{A,R}(\lambda)=j_o+j_{max}\int_0^{\infty}\frac{H_R(\beta)}{1+\left(2\dfrac{\lambda-\lambda_o}{W_e}-\alpha\beta^2\right)^2}d\beta. \tag{7}$$

The most difficult integral to deal with is the microfield strength distribution function, because this is a multidimensional integral. A straightforward manner would be the estimates of multidimensional integral by Monte Carlo method of integration. The number of random samples of points must be large in order to achieve satisfactory accuracy. That would lead to increased processor time [16].

The second integral in Eq. (6) is the $j_{A,R}(\lambda)$ and it is evaluated by summation method. The third integral is evaluated by the Gauss-Hermite method with $\exp(-t^2)$ as a weight function. In this way the number of terms in the numerical sum is reduced in comparison with the summation methods. It must be noted that in cases where ($W_G>0.5W_e$) in Eq. (6) which are frequent physical situations in astrophysical plasmas [32], this method of integration is not applicable. Then, the integration must be done by classical summation methods, which greatly slow down the iteration process, but these methods are the only correct ones, in this matter. The W_G is defined with Eq. (8) [i.e., Eq. (2.3) in Ref. [15]],

$$W_G=2\sqrt{\frac{2(\ln 2)kT}{m}}\frac{\lambda_o}{c}. \tag{8}$$

Here, T is the emitter equivalent kinetic temperature, m is its mass, and k and c are the Boltzmann constant and the velocity of light, respectively.

In general, the base line K_o in Eq. (6) is a function of wavelength. In many cases it is nearly constant, or linear function. We have included in our procedure the fitting of background by a cubic polynomial, as an independent step, in order to prepare experimental data for the main deconvolution procedure.

In this way Eq. (6) be solved, and now it can start with the fitting procedure itself. For Eq. (6), the fitting procedure will give the values for W_G, W_e, λ_o, R, A, and $K_{\max}$.

We use the standard manner of defining the best fit: the sum of the squares of the deviations (chi-square) of the theoretical function from their experimental points is at its minimum. In other words, we look for the global minimum of the chi-square function which is a hypersurface of n dimensions in a hyperspace of $n+1$ dimensions, where n is equal to a number of parameters for appropriate theoretical function. n is equal to six for the "K" profile.

The necessary condition for the minimum of chi-square sum is that the partial derivatives of the function are equal to zero. Therefore, in the case of K function we have a system of six nonlinear homogeneous equations with six parameters. We look for the numerical solutions of these systems by using the well-known Newton's method of successive approximations [15].

The seeking for the numerical solution of this problem by employing the computer is accompanied by a number of numerical difficulties. The Newton's method requires successive solving of the inverse Jacobi matrices of the system of

TABLE I. The Kr I line broadening characteristics. Our measured: total Stark FWHM ($W_t^{expt.}$ in pm within ±12% accuracy), electron Stark width ($W_e^{expt.}$ in pm within ±12% accuracy), ion (Kr II + Kr III) Stark width ($W_i^{expt.}$ in pm within ±12% accuracy), static ion broadening parameter ($A^{expt.}$, dimensionless within ±15% accuracy), and ion-dynamic coefficient ($D^{expt.}$, dimensionless within ±20% accuracy) at measured electron temperature ($T^{expt.}$) and electron density ($N^{expt.}$). $W_e^{theor.}$ denote our calculated electron Stark widths (see Table II). "Ref." represents experimental values given in this work (Tw) and those used from other authors: SKS, Ref. [11]; EMZ, Ref. [5]; KM, Ref. [10]; BHN, Ref. [6]; LAM, Ref. [9]; VS, Ref. [7]; UK, Ref. [8]. Transitions and wavelengths are taken from Refs. [14,38]. The asterisk denotes Stark widths calculated by us on the basis of the given $W_e^{expt.}$ and $A^{expt.}$ values at plasma parameters presented in Ref. [11] using Eqs. (1)–(3).

Transition	Multiplet	λ (nm)	$T^{expt.}$ (10^4 K)	$N^{expt.}$ (10^{22}m^{-3})	$W_t^{expt.}$ (pm)	$W_e^{expt.}$ (pm)	$W_i^{expt.}$ (pm)	$A^{expt.}$	$D^{expt.}$	Ref.	$W_e^{theor.}$ (pm)	$W_e^{expt.}/W_e^{theor.}$
$5s$-$5p$	$[3/2]_1^o-[1/2]_o$	758.741	1.7	16.5	177.5	164.4	13.1	0.074	1.46	Tw	255.8	0.64
			1.0	1.0	11.3*	10.1	1.2*	0.049		SKS	13.8	0.73
			1.3	1.0		14.6				EMZ	14.7	0.99
	$[3/2]_2^o-[3/2]_2$	760.154	1.7	16.5	157.6	146.4	11.2	0.071	1.53	Tw	196.4	0.80
			1.0	1.0	9.7*	8.6	1.1*	0.047		SKS	10.3	0.84
			1.3	1.0		16.0				EMZ	10.9	1.47
	$[3/2]_2^o-[3/2]_1$	769.454	1.7	16.5	130.8	121.8	9.0	0.068	1.65	Tw	191.4	0.64
			1.0	1.0	8.9*	8.0	0.9*	0.045		SKS	9.9	0.80
	$[3/2]_1^o-[3/2]_2$	819.005	1.7	16.5	172.8	160.7	12.1	0.070	1.56	Tw	226.0	0.71
			1.0	1.0	10.8*	9.6	1.2*	0.046		SKS	11.8	0.82
			1.3	1.0		14.8				EMZ	12.6	1.17
	$[3/2]_1^o-[3/2]_1$	829.811	1.7	16.5	165.5	154.2	11.3	0.068	1.60	Tw	217.8	0.71
			1.0	1.0	10.5*	9.4	1.1*	0.045		SKS	11.4	0.82
			1.3	1.0		14.7				EMZ	12.3	1.20
	$[3/2]_2^o-[5/2]_3$	811.290	1.7	16.5	169.7	157.6	12.1	0.071	1.56	Tw	193.0	0.82
			1.0	1.0	11.1*	9.9	1.2*	0.047		SKS	10.1	0.98
			1.3	1.0		13.3				EMZ	10.8	1.23
	$[3/2]_2^o-[5/2]_2$	810.436	1.7	16.5	189.2	175.2	14.0	0.074	1.50	Tw	194.7	0.90
			1.0	1.0	12.7*	11.3	1.4*	0.049		SKS	10.1	1.12
$5s$-$5p'$	$[3/2]_2^o-[1/2]_1$	557.029	1.7	16.5	156.9	145.8	11.1	0.070	1.25	Tw		
			1.0	10.0		96.0				KM		
			1.2	1.0		6.3				BHN		
			1.1	10.0		86.0				LAM		
	$[3/2]_2^o-[3/2]_2$	556.222	1.7	16.5	137.3	127.6	9.7	0.070	1.30	Tw		
			1.2	1.0		5.6				BHN		
	$[3/2]_1^o-[3/2]_2$	587.091	1.7	16.5	140.0	130.0	10.0	0.071	1.34	Tw		
			1.0	10.0		122.0				KM		
			1.2	1.0		5.8				BHN		
			1.7	158.0		900.0				VS		
			1.3	102.0		680.0				UK		
$5s'$-$5p'$	$[1/2]_1^o-[1/2]_1$	828.105	1.7	16.5	170.5	158.5	12.0	0.070	1.58	Tw		
	$[1/2]_1^o-[1/2]_o$	768.525	1.7	16.5	154.3	143.1	11.2	0.073	1.55	Tw		
			1.0	1.0	10.5*	9.4	1.1*	0.048		SKS		
			1.3	1.0		179.0				EMZ		
	$[1/2]_o^o-[1/2]_1$	785.482	1.7	16.5	161.0	149.8	11.2	0.069	1.56	Tw		
			1.0	1.0	10.1*	9.0	1.1*	0.046		SKS		
			1.3	1.0		154.0				EMZ		
	$[1/2]_1^o-[3/2]_2$	826.324	1.7	16.5	170.0	157.9	12.1	0.071	1.58	Tw		
			1.0	1.0	11.8*	10.6	1.2*	0.047		SKS		
	$[1/2]_o^o-[3/2]_1$	805.95	1.7	16.5	149.1	139.1	10.0	0.066	1.63	Tw		
			1.0	1.0	9.3*	8.4	0.9*	0.044		SKS		
			1.3	1.0		109.0				EMZ		

TABLE I. (*Continued*).

Transition	Multiplet	λ (nm)	$T^{\text{expt.}}$ (10^4 K)	$N^{\text{expt.}}$ (10^{22}m^{-3})	$W_t^{\text{expt.}}$ (pm)	$W_e^{\text{expt.}}$ (pm)	$W_i^{\text{expt.}}$ (pm)	$A^{\text{expt.}}$	$D^{\text{expt.}}$	Ref.	$W_e^{\text{theor.}}$ (pm)	$W_e^{\text{expt.}}/W_e^{\text{theor.}}$
$5s$-$6p$	$[3/2]_2^o-[1/2]_1$	436.264	1.7	16.5	342.8	325.2	17.6	0.050	1	Tw	389.4	0.84
	$[3/2]_2^o-[3/2]_2$	427.397	1.7	16.5	448.8	423.7	25.1	0.055	1	Tw	392.7	1.08
			1.1	10.0		275.0				LAM	223.0	1.23
	$[3/2]_1^o-[3/2]_1$	446.369	1.7	16.5	367.2	348.3	18.9	0.050	1	Tw	414.2	0.84
			1.1	10.0		263.0				LAM	234.0	1.12
	$[3/2]_2^o-[5/2]_3$	431.958	1.7	16.5	345.9	328.0	17.9	0.050	1	Tw	381.2	0.86
			1.2	1.0		27.0				BHN	21.8	1.24
$5s'$-$6p'$	$[1/2]_1^o-[1/2]_o$	435.136	1.7	16.5	495.6	469.9	25.7	0.051	1	Tw		

equations for each step, which are error prone due to the errors of rounding. Moreover, the numerical partial derivatives in Jacobi matrix itself are sources of errors of rounding. These errors of rounding destabilize the convergence of solution of the system, although the all-mathematical conditions are fulfilled. The algorithm may be stabilized by reducing the iteration procedure to independent parameters only, by neglecting the nondiagonal elements of Jacobi matrix. By this simplification the errors of rounding in inverse Jacobi matrix calculation decrease. Further stabilization of iterative process may be achieved by weighing the nondiagonal elements of inverse Jacobi matrix by real numbers in the domain (0, 1]. These modifications of Newton's method do not spoil the conditions of convergence and uniqueness of mathematical solution, but affect somewhat the speed of convergence. In this way we have contrived to give numerical solutions for fitting functions with more than three free parameters, which is difficult for nonpolynomial fits.

This sophisticated deconvolution method, which allows direct determining of all six parameters by fitting theor.etical *K*-profile [Eq. (6)], on experimental data, requires sufficient number of experimental points per line, and small statistical errors. The upper limits of numerical conditionality of this method are minimum twenty experimental points per line [the border of line is $(-3/2W_e+\lambda_o<\lambda<+3/5W_e+\lambda_o)$, where W_e is electron FWHM], and maximal statistical indeterminacy in intensity is 5% at every experimental point. Poor experimental measurements weaken the conditionality of the system of equations, and lead to nonapplicability of this method. This has been concluded by testing the sensitivity of the algorithm by generating random statistical noise with Gaussian distribution in every point involved in theor.etical profiles.

V. METHOD OF CALCULATION

The description of the semiclassical perturbation formalism is given in Refs. [20–25,33]. Within this formalism, Stark full-width (W) at the intensity half maximum (FWHM) and shift (d) of an isolated spectral line, may be expressed as [20,21]

$$W=N\int vf(v)dv\left(\sum_{i'\neq i}\sigma_{ii'}(v)+\sum_{f'\neq f}\sigma_{ff'}(v)+\sigma_{el}\right),$$

$$d=N\int vf(v)dv\int_{R_3}^{R_D}2\pi\rho d\rho\sin 2\phi_p, \tag{9}$$

where N is the electron density, $f(v)$ the Maxwellian velocity distribution function for electrons, ρ denotes the impact parameter of the incoming electron, i and f denote the initial and final atomic energy levels, and i', f' their corresponding perturbing levels. The inelastic cross section $\sigma_{j,j'}(v)$ can be expressed by an integral over the impact parameter of the transition probability $P_{jj'}(\rho,v)$ as

$$\sum_{j'\neq j}\sigma_{jj'}(v)=\frac{1}{2}\pi R_1^2+\int_{R_1}^{R_D}\sum_{j\neq j'}P_{jj'}(\rho,v),j=i,f \tag{10}$$

and the elastic cross section is given by

$$\sigma_{el}=2\pi R_2^2+\int_{R_2}^{R_D}8\pi\rho d\rho\sin^2\delta,$$

$$\delta=(\phi_p^2+\phi_q^2)^{1/2}. \tag{11}$$

The phase shifts ϕ_p and ϕ_q due, respectively, to the polarization potential (r^{-4}) and to the quadrupolar potential (r^{-3}), are given in Sec. 3 of Chap. 2 in Ref. [20]. R_D is the Debye radius. All the cutoffs R_1, R_2, R_3 are described in Sec. 1 of Chap. 3 in Ref. [21].

For electrons hyperbolic paths due to the attractive Coulomb force were used, while for perturbing ions the paths are different since the force is repulsive. The formulas for the ion-impact widths and shifts are analogous to Eqs. (9)–(11). The difference in calculation of the corresponding transition probabilities and phase shifts as a function of the impact parameter in Eqs. (10) and (11) is in the ion perturber trajectories which are influenced by the repulsive Coulomb force instead of an attractive one as for electrons.

Energy levels have been taken from Ref. [34]. Oscillator strengths have been calculated by using the method of Bates and Damgaard [35,36]. For higher levels, the method described in Ref. [37] has been used. It is not possible to perform semiclassical calculation in an adequate way for experi-

TABLE II. Calculated Kr I Stark FWHM ($W^{\text{theor.}}$ in pm) for electrons (a), protons (b), and helium ions (c) as perturbers for various temperatures (T) at 10^{22} m^{-3} perturber density.

λ (nm)		T (10^3 K)					
		2.5	5.0	10.0	20.0	30.0	50.0
758.741	a	10.6	12.2	13.8	16.4	18.1	21.0
	b	4.10	4.25	4.42	4.63	4.78	4.99
	c	3.89	4.01	4.12	4.26	4.36	4.50
760.154	a	8.22	9.12	10.3	12.6	14.4	17.2
	b	3.51	3.60	3.69	3.81	3.90	4.02
	c	3.40	3.47	3.53	3.61	3.66	3.74
769.454	a	7.91	8.76	9.88	12.2	13.9	16.8
	b	3.50	3.57	3.66	3.76	3.83	3.94
	c	3.40	3.46	3.52	3.58	3.63	3.70
819.005	a	9.38	10.4	11.8	14.6	16.8	20.2
	b	4.06	4.15	4.26	4.39	4.49	4.62
	c	3.94	4.01	4.08	4.17	4.22	4.31
829.811	a	9.04	9.98	11.4	14.1	16.3	19.8
	b	4.05	4.14	4.23	4.34	4.42	4.54
	c	3.95	4.02	4.08	4.15	4.20	4.27
811.290	a	8.26	8.94	10.1	12.5	14.6	17.8
	b	3.59	3.66	3.74	3.84	3.90	4.00
	c	3.50	3.56	3.61	3.67	3.71	3.78
810.436	a	8.25	8.93	10.1	12.5	14.6	17.8
	b	3.59	3.66	3.74	3.83	3.90	4.00
	c	3.50	3.56	3.61	3.67	3.71	3.77
436.264	a	17.5	19.6	21.7	24.3	26.2	28.6
	b			6.17	6.58	6.86	7.27
	c					6.06	6.32
427.397	a	17.3	19.9	22.0	24.5	26.1	28.6
	b			6.42	6.84	7.12	7.54
	c						6.55
446.369	a	18.1	20.7	23.1	25.8	27.6	30.4
	b			6.83	7.25	7.54	7.96
	c						6.96
431.958	a	16.7	19.0	21.2	23.9	25.8	28.6
	b			6.17	6.54	6.79	7.16
	c						6.31

mental spectral lines originating from transitions involving $5p'[1/2]$, $5p'[3/2]$, $6p'[1/2]$, and $6p'[3/2]$ energy levels, since experimental data for $nd'[1/2]$ energy levels are missing. The expected accuracy of the semiclassical perturbation approach is $\pm 30\%$. However, due to the complexity of krypton spectrum and missing atomic energy levels, we expect that the accuracy of calculated Stark widths is $\pm 40\%$ for transitions from $5p$ levels and even $\pm 45\%$ from transitions involving $6p$ levels.

VI. RESULTS AND DISCUSSION

Our experimentally obtained $W_t^{\text{expt.}}$, $W_e^{\text{expt.}}$, $W_i^{\text{expt.}}$, $A^{\text{expt.}}$, and $D^{\text{expt.}}$ data are presented in Table I.

Calculated Stark FWHM values ($W^{\text{theor.}}$) generated by electrons, protons and helium ions for eleven Kr I lines in the $5s$-$5p$ and $5s$-$6p$ transitions using SCPF are presented in Table II.

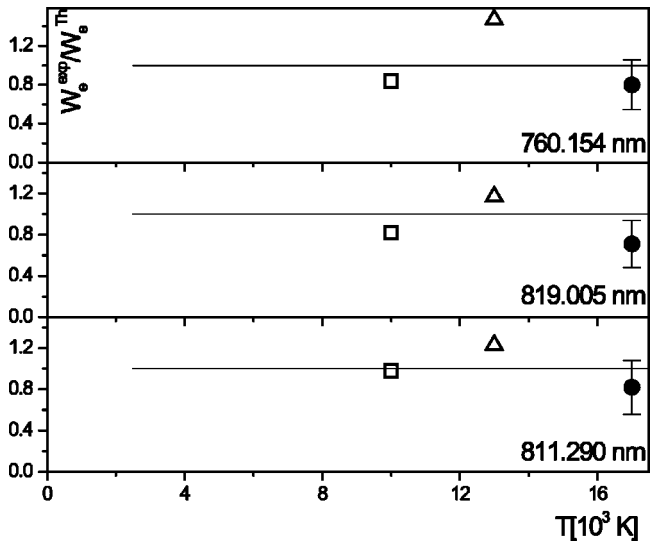

FIG. 3. Ratios of the experimental $W_e^{\text{expt.}}$ and our calculated $W_e^{\text{theor.}}$ electron Stark widths vs electron temperature for the most investigated Kr I spectral lines belonging to the $5s$-$5p$ transition. ●, our experimental results and those of other authors: □, Ref. [11] and △, Ref. [5]. Error bars ($\pm 30\%$) include the uncertainties of the width ($\pm 12\%$), electron density ($\pm 7\%$), and temperature ($\pm 11\%$) measurements.

The measured $N^{\text{expt.}}$ and $T^{\text{expt.}}$ decays are presented in Fig. 2, together with the averaged (within 20 Kr I lines) N^{D} and T^{D} values obtained using the line profile deconvolution procedure for Kr I lines. One can conclude that the agreement among $N^{\text{expt.}}$ and N^{D} values is very good (within 7% on average). This fact confirms homogeneity of investigated plasma in the linear part of our light source (see Fig. 1 in Ref. [26]). In the case of the electron density, the situation is similar. The agreement among the two sets of the electron temperature decays ($T^{\text{expt.}}$ and T^{D}) is between the experimental accuracy of $\pm 11\%$ and uncertainties ($\pm 12\%$) of the results obtained by deconvolution procedure.

Existing experimental Stark width values ($W_e^{\text{expt.}}$) are compared to our measured and calculated ($W_e^{\text{theor.}}$) data (see Table I and Fig. 3).

The EMZ [5] and LAM [9] $W_e^{\text{expt.}}$ values lie above our calculated ones for about 25% and 17%, respectively.

Our $W_e^{\text{expt.}}/W_e^{\text{theor.}}$ is 0.82 (on average) except 758.741-nm and 769.454-nm lines for which 0.64 was found. The agreement between our measured and calculated (W_e) values is better for the lines in highly lying ($5s$-$6p$) transition.

$W_e^{\text{expt.}}$ values from Ref. [11] agree well with our calculated ones. Thus, the ratio $W_e^{\text{expt.}}/W_e^{\text{theor.}}$ for values from Ref. [11] is 0.86 (averaged within seven lines).

In the case of the most investigated 587.091-nm Kr I line, the comparison among experimental values is not possible due to various plasma parameters at which they are determined.

We have found that the ion contribution (Kr II + Kr III) to the total ($W_t^{\text{expt.}}$) Stark width is about 8% for the $5s$-$5p$

transitions and about 5% for the $5s$-$6p$ transitions.

It turns out that the ratio between our $W_i^{\text{expt.}}$ values and those from Ref. [11] is constant ($10 \pm 24\,\%$) for 11 Kr I lines. Furthermore, this ratio has approximately the same value as the ratio between the factors of N/T in the two experiments ($9.7 \pm 18\,\%$).

We have found that the Stark widths ($W^{\text{theor.}}$) generated by protons and helium ions are mutually close and are two or four times smaller than the widths generated by electrons and practically independent of T up to 50 000 K (see Table II).

Our $A^{\text{expt.}}$ values can be separated into two groups. In the first group are the higher A values (from 0.067 up to 0.074) corresponding to the lines in the $5s$-$5p$ transitions. The second group comprises the lower A values (from 0.050 up to 0.055) corresponding to the lines in the higher lying $5s$-$6p$ transitions.

It turns out that our $A^{\text{expt.}}$ values show small internal scatter within the mentioned groups. They lie within $\pm 7\%$ of the mean value. A similar behavior is also shown by A values from Ref. [11] in the $5s$-$5p$ transitions. Their scatter is $\pm 6\%$.

The normalized A values obtained in Ref. [11] (taking the $N^{1/4}$ normalization factor from Ref. [29]) are about 34% higher than ours. But, taking into account the difference between electron temperatures (10 000 K and 17 000 K) in the two experiments, this discrepancy is really lower than 34% and can be estimated to be 20%. Thus, one can conclude that tolerable agreement exists among our A values and those from Ref. [11].

It should be pointed out that our A values in the Kr I $5s$-$6p$ transitions are the unique data in this field. We have found that the ion-dynamic effect plays a significant role in the Kr I line broadening (at our plasma conditions) and multiplies the quasistatic ion effect by about 1.5 times (on average) in the case of the $5s$-$5p$ transition.

VII. CONCLUSION

We have found evident influence of the quasistatic ion and ion-dynamic effects on the investigated Kr I spectral line shapes. Moreover, since conditions of validity of the impact and quasistatic approximation differ in Refs. [20,21] and in Ref. [29], experimental determinations of ion broadening contribution are of interest for their elaboration. It is shown that the line deconvolution procedure, described by Ref. [15], applied to Kr I line profiles, gives convenient plasma parameters (N and T, confirmed experimentally) at about 17 000 K electron temperature and 1.65×10^{23} m^{-3} electron density. We recommend this method for plasma diagnostical and modeling purposes.

ACKNOWLEDGMENTS

This work is a part of the projects ''Determination of the Atomic Parameters on the Basis of the Spectral Line Profiles'' and ''Influence of Collision Processes on Astrophysical Plasma Line Shapes'' supported by the Ministry of Science, Technologies and Development of the Republic of Serbia. S. Djeniže is grateful to the ''Arany János K'ózalapitvány,'' Budapest, Hungary.

[1] J.A. Cardelli, B.D. Savage, and D.C. Ebbets, Astrophys. J. **383**, L23 (1991).
[2] D. S. Leckrone, G. M. Wahlgren, S. G. Johansson, and S. J. Adelman, in *Peculiar versus Normal Phenomena in A-type and Related Stars,* International Astronomical Union Colloquium No. 138, Trieste, 1992, edited by M. M. Dworetsky, F. Castelli, and R. Faraggiana (Astronomical Society of the Pacific, San Francisco, 1993).
[3] D.S. Leckrone *et al.*, ASP Conf. Ser. **44**, 42 (1993).
[4] H.L. Dinerstein, Astrophys. J. **550**, L223 (2001).
[5] W.E. Ernst, B.H. Müller, and T. Zaengel, Physica C **93**, 414 (1978).
[6] T. Brandt, V. Helbig, and K. Nick, in *Proceedings of ICSLS, 1981*, edited by B. Wende (W. de Gruyter, Berlin, 1981), p. 265.
[7] Y. Vitel and M. Skowronek, J. Phys. B **20**, 6493 (1987).
[8] N.I. Uzelac and N. Konjević, J. Phys. B **22**, 2517 (1989).
[9] A. Lesage, D. Abadie, and M.H. Miller, Phys. Rev. A **40**, 1367 (1989).
[10] P. Klein and D. Meiners, J. Quant. Spectrosc. Radiat. Transf. **17**, 197 (1977).
[11] D. Schinköth, M. Kock, and E. Schultz-Gulde, J. Quant. Spectrosc. Radiat. Transf. **64**, 635 (2000).
[12] A. Lesage and J. R. Fuhr (unpublished).
[13] N. Konjević *et al.*, J. Phys. Chem. Ref. Data **31**, 819 (2002).
[14] NIST (2002), Atomic Spectra Data Base Lines, http://physics.nist.gov .
[15] V. Milosavljević and G. Poparić, Phys. Rev. E **63**, 036404 (2001).
[16] V. Milosavljević, Ph.D. thesis, University of Belgrade, Faculty of Physics, Belgrade, 2001 (unpublished).
[17] V. Milosavljević and S. Djeniže, Astron. Astrophys. **393**, 721 (2002).
[18] V. Milosavljević and S. Djeniže, New Astron. **7/8**, 543 (2002).
[19] V. Milosavljević and S. Djeniže, Phys. Lett. A **305/1-2**, 70 (2002).
[20] S. Sahal-Bréchot, Astron. Astrophys. **1**, 91 (1969).
[21] S. Sahal-Bréchot, Astron. Astrophys. **2**, 322 (1969).
[22] S. Sahal-Bréchot, Astron. Astrophys. **35**, 321 (1974).
[23] M.S. Dimitrijević and S. Sahal-Bréchot, J. Quant. Spectrosc. Radiat. Transf. **31**, 301 (1984).
[24] M.S. Dimitrijević and S. Sahal-Bréchot, Phys. Rev. A **31**, 316 (1985).
[25] M.S. Dimitrijević, S. Sahal-Bréchot, and V. Bommier, Astron. Astrophys., Suppl. Ser. **89**, 581 (1991).
[26] S. Djeniže, V. Milosavljević, and A. Srećković, J. Quant. Spectrosc. Radiat. Transf. **59**, 71 (1998).
[27] V. Milosavljević *et al.*, Phys. Rev. E **62**, 4137 (2000).
[28] S. Djeniže and S. Bukvić, Astron. Astrophys. **365**, 252 (2001).
[29] H. R. Griem, *Spectral Line Broadening by Plasmas* (Academic Press, New York, 1974).

[30] A.J. Barnard, J. Cooper, and E.W. Smith, J. Quant. Spectrosc. Radiat. Transf. **14**, 1025 (1974).
[31] D.E. Kelleher, J. Quant. Spectrosc. Radiat. Transf. **25**, 191 (1981).
[32] L.Č. Popović, M.S. Dimitrijević, and D. Tankosić, Astron. Astrophys., Suppl. Ser. **139**, 617 (1999).
[33] C. Fleurier, S. Sahal-Bréchot, and J. Chapelle, J. Quant. Spectrosc. Radiat. Transf. **17**, 595 (1977).
[34] J. Sugar and A. Musgrove, J. Phys. Chem. Ref. Data **20**, 859 (1991).
[35] D.R. Bates and A. Damgaard, Philos. Trans. R. Soc. London, Ser. A **242**, 101 (1949).
[36] H. VanRegemorter, Dy. HoangBinh, and M. Prud'homme, J. Phys. B **12**, 1053 (1979).
[37] G.K. Oertel and L.P. Shomo, Astrophys. J., Suppl. Ser. **16**, 175 (1968).
[38] R. A. Striganov and N. S. Sventickij, *Tablicy Spektral'nykh linij* (Atomizdat, Moskva, 1966).